DANISH METEOROLOGICAL INSTITUTE

SCIENTIFIC REPORT

99-5

Non-Linear High Resolution Inversion of Radio Occultation Data

Mette Dahl Mortensen

DMI

COPENHAGEN 1999

ISSN-Nr. 0905-3263
ISSN-Nr. 1399-1949 (Online)
ISBN-Nr. 87-7478-392-0

Non-Linear High Resolution Inversion of Radio Occultation Data

Mette Dahl Mortensen

Danish Meteorological Institute
Denmark

February, 1999

Contents

1 Introduction

The global positioning system (GPS) is a system of satellites placed at an altitude of $26000km$. The system is used for precise positioning on the Earth. The GPS satellites transmit radio signals with a very well defined phase. When a receiver measures this signal the position of the receiver relative to the GPS satellite can be determined by calculating the phase delay of the signal. The phase delay is caused by the propagation from the GPS to the receiver and is thus equivalent to a time delay.

When the receiver is placed on board a low Earth orbiting satellite (LEO) the signal will propagate horizontally through the atmosphere of the Earth. This is illustrated in Figure 1. The LEO is placed at an altitude of $800km$. The signal will propagate as illustrated by the ray path.

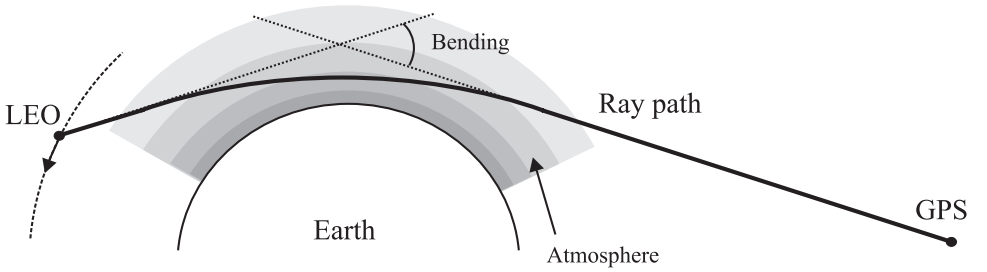

Figure 1: The geometry of the occultation.

The atmosphere of the Earth is approximately locally spherically symmetric and the density decreases exponentially with altitude. The propagation through the atmosphere will introduce a further phase delay compared to the one seen in free space propagation. Also the signal will not propagate in a straight line but rather be bend. As the density decreases the signal delay and bending will decrease accordingly.

If the position of the GPS and the LEO satellite is known the phase delay measured by the LEO satellite contains information about the atmosphere. The principle in an radio occultation measurement is to measured the change in the delay measured by the LEO as the LEO sets behind the limb of the Earth relative to the GPS satellite. The amplitude of the received signal in principle contains the same information as the phase but is less precise.

The radio occultation measurement can be inverted to give information on the density, pressure and temperature of the atmosphere. To do this a model for the signal propagation must be made. The signal has a frequency of $L_1 = 1.227Ghz$ or $L_2 = 1.572GHz$ - both frequencies are transmitted and received. The model used should thus be an electromagnetic wave propagation model.

When inverting radio occultation measurements of the atmosphere of the Earth a geometrical optics approach is usually taken. In this approximation the wave propagation is approximated by rays. The geometrical optics approximation is valid in the limit $\lambda \to 0$ where λ denotes the wavelength. This is usually a good approximation but due to the vertical gradient in the refractive index in the atmosphere the vertical resolution obtained by using the geometrical optics

approximation will be diffraction limited. Diffraction is seen when the wavelength is finite and causes the ray to spread out as the signal propagates, thus, the signal will be defocused and the resolution decreased. The geometrical optics inversion method further more assumes that the atmosphere is spherically symmetric.

Alternative inversion methods are based on full wave propagation methods but due to the very large propagation distance it is necessary to introduce several approximations in the models. One such method is described in the following. The method has the potential for high vertical resolution and avoidance of the spherical symmetry assumption.

2 The nonlinear high resolution inversion method

2.1 The geometry

A schematic illustration of the model of the occultation geometry is shown in Figure 2.

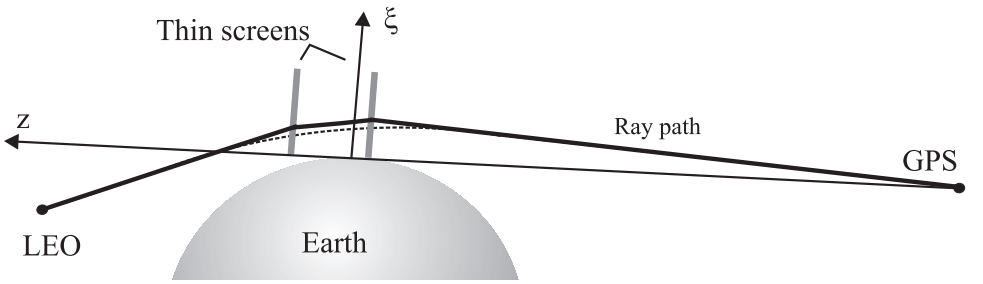

Figure 2: The two screen approximation of an occultation.

For each sample in the occultation measurement a coordinate system (z, ξ) is defined in the plane given by the position of the GPS and the LEO satellites and the center of the Earth. The $z-$axis is the vector from the GPS satellite tangential to the Earth closest to the LEO satellite. The $\xi-$axis is perpendicular to the Earth at the tangent point.

This two dimensional approximation can be used under the assumption that the horizontal structures in the atmosphere are large compared to the lateral dimensions of the Fresnel zone. The Fresnel zone is a measure of the area which has influence on the measurement. In an occultation measurement of the Earth the Fresnel zone size is less than 2km so the two dimensional approximation is normally good.

The dashed line illustrates the actual ray path which approximates the propagation of signal. The model uses two thin screens to model the atmosphere. At each thin screen a phase delay due to atmosphere is added and the signal is bend. In between the screens and to and from the screens the signal is assumed to propagate in free space. As can be seen from Figure 2 this will introduce an approximation of the length of the signal propagation path. As long as the bending of the signal is relatively small the error originating from this approximation will be

negligible. It has previously been shown that use of a single thin screen to model the atmosphere gives promising results [Mortensen and Høeg, 1998] and use of two screens is expected to give better results. It is not clear from beforehand whether the expected improvement is sufficient to comply with the very high accuracy demands for atmospheric measurements, but conceptually the model can easily be extended to include more screens once the improvement of introducing the extra thin screen has been proven.

2.2 Propagation

The complex amplitude u of the scalar electro-magnetic field in vacuum satisfies the Helmholtz equation

$$\Delta u + k^2 u = 0 \tag{1}$$

where k is the free space wave number. The scalar version of the wave equation can be used because the atmosphere is tenuous [Tartarskii, 1971].

If the electro-magnetic field u_0 is known at a distant straight line S a solution $u(\vec{x})$ to the Helmholtz equation can be found in a given point $\vec{x}$. This is the two dimensional solution for the external boundary problem for the Helmholtz equation [Born and Wolf, 1993]

$$u(\vec{x}) = \frac{i}{2} \int_S u_0(\vec{y}) \frac{\partial}{\partial n_y} H_0^{(1)}(k|\vec{x} - \vec{y}|)\, dS_y \tag{2}$$

where n_y is the external normal to S and $H_0^{(1)}$ is the Hankel function of first kind of zero order.

When using the high frequency expansion $(k|\vec{x} - \vec{y}|) \to \infty$ of $H_0^{(1)}$, the expression for the field becomes

$$u(\vec{x}) = \left(\frac{k}{2\pi}\right)^{1/2} \int_S u_0(\vec{y}) \cos\varphi_{xy} \frac{\exp(ik|\vec{x} - \vec{y}| - i\pi/4)}{\sqrt{|\vec{x} - \vec{y}|}}\, dS_y \tag{3}$$

where φ_{xy} is the angle between the normal $\vec{n}_y$ to S and the vector $\vec{x} - \vec{y}$. This solution can be used to describe the field measured at the LEO if the field is known on the thin screens (ξ, z_0) indicated in Figure 2.

As the signal propagates in free space from the GPS satellite to the first thin screen the field u_1 at this will be given as

$$u_1(\xi, z_1) = u_G \frac{\exp(ikr_{G,1})}{\sqrt{r_{G,1}}} \exp(ik\psi(\xi)). \tag{4}$$

In this equation, u_G denotes the field transmitted from the GPS, $r_{G,1}$ is the distance from the GPS to the point (ξ, z_1) in the thin screen and ψ is the phase delay due to the atmosphere.

The field at the second thin screen will then be

$$u_2(\xi, z_2) = \sqrt{\frac{k}{2\pi}} \exp(ik\psi(\xi)) \int_{-\infty}^{\infty} u_1(\xi', z_1) \cos\varphi_{1,2} \frac{\exp(ikr_{1,2} - i\pi/4)}{\sqrt{r_{1,2}}}\, d\xi' \tag{5}$$

using (3) and (4). In this case $r_{1,2}$ denotes the distance between the points (ξ, z_1) and (ξ, z_2) and $\varphi_{1,2}$ is the angle between the vector $\vec{r}_{1,2}$ and the z-axis.

Reusing (3) the field measured by the LEO can be determined as

$$u_L(\vec{r}_L) = \left(\frac{k}{2\pi}\right)^{1/2} \int_{-\infty}^{\infty} u_2(\xi, z_2) \cos\varphi_{2,L} \frac{\exp(ikr_{2,L} - i\pi/4)}{\sqrt{r_{2,L}}}\, d\xi \tag{6}$$

when (5) is used for the field u_2. Here $r_{2,L}$ denotes the distance between the points (ξ, z_2) and $\vec{r}_L$ and $\varphi_{2,L}$ is the angle between the vector $\vec{r}_{2,L}$ and the z-axis.

The expressions have been written using thin screens parallel with the ξ-axis but the expressions can easily be generalized to include a slope compared to the ξ-axis. At both thin screens the field will be zero below the surface of the Earth.

The propagation method assumes stationarity in time as the occultation samples used to calculate the field are in reality a time series. This is a good approximation for the atmosphere as the occultation measurement only takes about a minute during which time interval the atmosphere can not change significantly.

The phase delay ψ due to the atmosphere is found using a geometrical optics approximation and using an assumption of spherical symmetry in the atmosphere. This is not limiting for the results though as the geometrical optics approximation is a good approximation when the area for which it is used is relatively small. In the case case here it is only used to find the phase delay due to the atmosphere and the spherical symmetry assumption becomes local, i.e., must only be valid in the vicinity of each screen. For each screen the phase delay will be given as [Born and Wolf, 1993]

$$\psi_i(\xi) = \int_{\xi+R_E}^{\infty} (n_i - 1) \frac{n_i r}{\sqrt{n_i^2 r^2 - a^2}}\, dr \tag{7}$$

where n_i is the refractive index (proportional to the density) in the part of the atmosphere corresponding to screen number $i = 1, 2$ and $a = n_i(\xi)(\xi + R_E)$. R_E denotes the radius of the center of refractivity for the Earth [Syndergaard, 1998]. Figure 3 illustrates the parameters used for calculating the phase delay ψ_i.

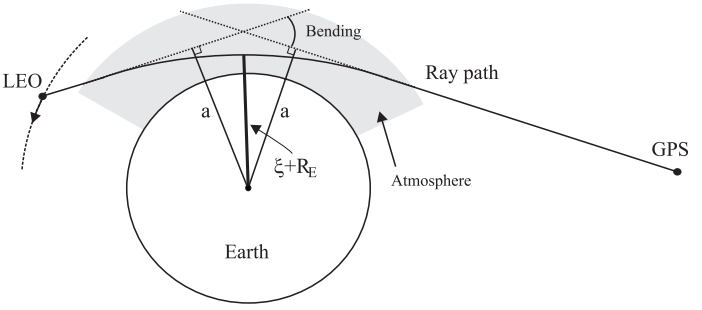

Figure 3: The occultation geometry.

2.3 Inversion

In an occultation measurement the electromagnetic field is measured in the form of amplitude and phase of the signal sent from the GPS. The information wanted from the measurements are temperature, pressure and density profiles. These quantities are proportional to the refractive index, i.e., the purpose of the inversion here is to derive refractive index profiles from the occultation measurement.

It is obvious to split the inversion in two parts: Calculation of phase delay ψ_i from the measured phase and calculation of refractive index from phase delay. In the formulation given in the previous section both will be nonlinear inversions.

As an occultation measurement gives a one-dimensional data set some a priori information about the horizontal variations in the refractive index is necessary if $\psi_1 \neq \psi_2$. To keep the inversion as simple as possible it has thus been assumed that the atmosphere is spherically symmetric, i.e., $\psi_1 = \psi_2 = \psi$. Once the inversion works for a spherically symmetric atmosphere the extension to $\psi_1 \neq \psi_2$ should conceptually be a minor extension.

Calculation of the refractive index from the phase delay can be performed analytically. An approximation for the expression (7) is

$$\psi(\xi) = -\int_{\xi}^{\infty} \frac{(dn/dr)}{n_i} \sqrt{n^2 r^2 - a^2}\, dr \tag{8}$$

The approximation is valid for a tenuous atmosphere ($n \approx 1$) which is a good approximation for the Earth especially when the atmosphere is departed in to two or more parts. This expression can be inverted giving

$$n(a) = \exp\left(-\frac{1}{2\pi} \frac{d}{da} \left[\int_{a}^{\infty} \frac{a\psi(\xi_n - R_E)}{\xi_n \sqrt{\xi_n^2 - a^2}}\, d\xi \right] \right) \tag{9}$$

with $\xi = \frac{a}{n(a)} - R_E$ (after the inversion) and using $\xi_n = n(\xi + R_E) \approx \xi + R_E$. Use of the approximation $\xi_n \approx \xi + R_E$ is equal to a slight change in the propagation path. As $n > 1$ the ray path will be moved slightly outwards. From Figure 3 it can be seen that the approximation is equal to assuming that the distance to the center of the Earth at the thin screens is equal to a instead of $(\xi + R_E)$. As the distance from the satellites to the atmosphere of the Earth is a lot larger than the propagation distance within the atmosphere this gives the best approximation of the propagation path.

The inversion from measured field to phase delay can not be simplified in the same manner so this part is solved by discretizing and performing a nonlinear iterative inversion algorithm.

The propagation through the atmosphere of the Earth has influence on both the measured amplitude and phase. The approximation of the propagation to the two-thin screen model will thus also both have influence on phase and amplitude of the measurement. On the other hand the expression for the measured field as shown in (6) only contains an unknown phase. In order

to perform the nonlinear iterative inversion the expression is rewritten to better comply with the measured quantity:

$$u_L(\vec{r}_L) = K_L \int_{-\infty}^{\infty} \Psi(\xi) \frac{\exp(ikr_{2,L})}{\sqrt{r_{2,L}}} \cos\varphi_{2,L} \int_{-\infty}^{\infty} \Psi(\xi') \frac{\exp(ik(r_{G,1}+r_{1,2})}{\sqrt{r_{G,1}r_{1,2}}} \cos\varphi_{1,2}\, d\xi' d\xi \qquad (10)$$

where K_L is a complex constant and $\Psi(\xi) = A(\xi)\exp(ik\psi(\xi))$. Thus, the unknown to be derived is the complex quantity Ψ of which only the phase ψ is to be used to find the refractive index.

The expression (10) for the measured field will be inverted using Newton's method. The idea in this is to use an initial guess of the phase delay Ψ to calculate the two thin screen propagation solution and then a Taylor's expansion of the nonlinear equation is used to calculate an updating of the model for the unknown. The updated phase delay can then be used to calculate the two thin screen propagation and the steps can be repeated until convergence or not.

The operator equation which is to be solved for Ψ is written as

$$u_L(\vec{r}_L) = \mathcal{F}[\vec{r}_L, \Psi(\xi)]. \qquad (11)$$

A guess for the solution is $\Psi^{(k)}$. When this guess is not the exact solution Ψ a correction $\partial\Psi^{(k)}$ must be found such that the sum $\Psi + \partial\Psi^{(k)}$ is the correct solution, i.e.,

$$\mathcal{F}[\Psi^{(k)} + \partial\Psi^{(k)}] = u_L. \qquad (12)$$

The position dependencies $\vec{r}_L$ and ξ has been omitted in the equation and will be omitted in the following for the sake of simplicity.

The truncated Taylor expansion of equation (12) is

$$\mathcal{F}[\Psi^{(k)} + \partial\Psi^{(k)}] \simeq \mathcal{F}[\Psi^{(k)}] + \left(\frac{\partial\mathcal{F}}{\partial\Psi}\right)^{(k)} \partial\Psi^{(k)}. \qquad (13)$$

Thus, an updating equation, which will be likely to improve the guess is
[Blok and Oristaglio, 1995, ch. 3.4]

$$u_L - \mathcal{F}[\Psi^{(k)}] = \left(\frac{\partial\mathcal{F}}{\partial\Psi}\right)^{(k)} \partial\Psi^{(k)} \qquad (14)$$

and the updated result for the phase becomes

$$\Psi^{(k+1)} = \Psi^{(k)} + \partial\Psi^{(k)} \qquad (15)$$

where (k) denotes the iteration number.

The Taylor expansion truncated to the first order is not necessarily a good approximation of the nonlinear equation, particularly if the initial guess is far from the correct result. Thus, it is commonly used to regularize the updating solution $\partial\Psi^{(k)}$ in the sense that $\partial\Psi^{(k)}$ is chosen as [Blok and Oristaglio, 1995, ch. 3.4]

$$\min\left\{ \left\| u_L - \mathcal{F}[\Psi^{(k)} + \partial\Psi^{(k)}] \right\|_2^2 + \lambda^2 \left\| \partial\Psi \right\|_2^2 \right\}. \qquad (16)$$

In the present case this regularization has been done by trial and error. Thus, this aspect is treated in section 3 where the results are shown.

2.3.1 Solving the updating equations

The updating equation (14) is ill posed. Thus it must be solved using the least squares solution to the regularized problem [Hansen, 1997, ch. 1.3]:

$$\min \left\{ \left\| \left(\frac{\partial \mathcal{F}}{\partial \Psi} \right)^{(k)} \partial \Psi^{(k)} - \left(u_L - \mathcal{F}[\Psi^{(k)}] \right) \right\|_2^2 + \lambda^2 \left\| \partial \Psi \right\|_2^2 \right\} \tag{17}$$

As can be seen from the equation it has been chosen to minimize with respect to $\|\partial\Psi\|_2^2$. This is not necessarily the optimal choice of smoothing norm for the problem at hand but is used as an initial choice.

Even though the atmosphere of the Earth is tenuous the horizontally propagation path in an occultation makes the complex phase Ψ vary rather fast. Ψ will thus be an oscillating function with the number of oscillations increasing exponentially when the signal is approaching the Earth. It has been chosen to discretize this function by linear interpolation to make the calculation of the expansion functions reasonably simple. Due to the increasing number of oscillations the stepsize in the discretization must be variating with decreasing stepsize as the signal gets closer to the Earth. The discrete version of Ψ is thus,

$$\Psi(\xi) = \sum \phi_i \Phi_i(\xi) \text{ for } i = 1, \ldots, n \tag{18}$$

with

$$\Phi_i(\xi) = \begin{cases} \frac{1}{\xi_i - \xi_{i+1}}(\xi - \xi_{i+1}) & for\ \xi \in [\xi_{i+1}, \xi_i[\\ \frac{1}{\xi_{i-1} - \xi_i}(\xi_{i-1} - \xi) & for\ \xi \in [\xi_i, \xi_{i-1}] \\ 0 & otherwise. \end{cases} \tag{19}$$

The discretization scheme and the expansion functions are illustrated in Figure 4.

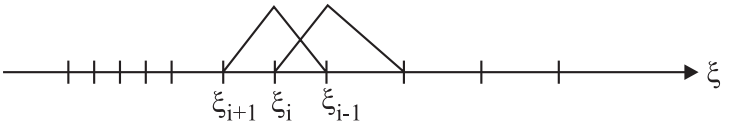

Figure 4: The expansion functions.

The discretization of the measurement is natural to perform as collocation, i.e., delta function expansions as this equals the samples in a measurement

$$v_j = u_L(\vec{r}_{L,j}) \text{ for } j = 1, \ldots, m \tag{20}$$

where $\vec{r}_{L,j}$ denotes the position for sample j. This sampling density increases as the Earth is approached. Similarly, the operator will be discretized in the same points $\mathbf{F}_j = \mathcal{F}[\vec{r}_{L,j}]$

The discretized equations are thus,

$$v_j = \mathbf{F}_j[\boldsymbol{\phi}^{(k)}] \text{ for } j = 1, \ldots, m \tag{21}$$

then the updating equations becomes

$$\upsilon_j - \mathbf{F}_j[\boldsymbol{\phi}^{(k)}] = \sum_{i=1}^{n} \left(\frac{\partial \mathbf{F}_j}{\partial \phi_i} \right)^{(k)} \partial \phi_i^{(k)} \text{ for } j = 1, \ldots, m \tag{22}$$

and the updated result for the phase becomes

$$\phi_i^{(k+1)} = \phi_i^{(k)} + \partial \phi_i^{(k)} \text{ for } i = 1, \ldots, n \tag{23}$$

The partial derivative of the measured field with respect to one of the expansion function is given as

$$\begin{aligned} \frac{\partial \mathbf{F}_j^{(k)}}{\partial \phi_i^{(k)}} = K_L \Bigg(& \int_{-\infty}^{\infty} \Phi_i(\xi) \frac{\exp(ikr_{2,L})}{\sqrt{r_{2,L}}} \cos\varphi_{2,L} \int_{-\infty}^{\infty} \Psi(\xi') \frac{\exp(ik(r_{G,1} + r_{1,2}))}{\sqrt{r_{G,1} r_{1,2}}} \cos\varphi_{1,2} \, d\xi' d\xi \\ & + \int_{-\infty}^{\infty} \Psi(\xi) \frac{\exp(ikr_{2,L})}{\sqrt{r_{2,L}}} \cos\varphi_{2,L} \int_{-\infty}^{\infty} \Phi_i(\xi') \frac{\exp(ik(r_{G,1} + r_{1,2}))}{\sqrt{r_{G,1} r_{1,2}}} \cos\varphi_{1,2} \, d\xi' d\xi \Bigg) \end{aligned} \tag{24}$$

Due to the unequal sampling density an appropriate weighting factor must be used in the discretization scheme to calculate $\|\partial\Psi\|_2$. The chosen expansion functions are not orthonormal so a direct normalization of the functions can not be done directly, instead the functions have been weighted according to their width to give them all the same influence, i.e., $w_i = \sqrt{\xi_{i-1} - \xi_{i+1}}$.

The updating equation (22) is not regular and further more it is ill posed. The discrete version of the least squares solution to the regularized problem thus looks like [Hansen, 1997, ch. 1.3]:

$$\min \left\{ \left\| \left(\frac{\partial \mathbf{F}}{\partial \boldsymbol{\phi}} \right) \partial \boldsymbol{\phi} - (\boldsymbol{\upsilon} - \mathbf{F}[\boldsymbol{\phi}]) \right\|_2^2 + \lambda^2 \left\| \mathbf{L} \partial \boldsymbol{\phi} \right\|_2^2 \right\} \tag{25}$$

where $\mathbf{L}$ is a diagonal matrix containing the weighting values w_i and the superscript (k) has been dropped.

As an occultation normally extends from $100km$ altitude to around the surface of the Earth the number of samples in one occultation is large, i.e., around 1500. Even with this number of samples the measured phase variation from sample to sample close to the Earth is larger than 2π. So, in order to get a good representation of the signal in complex notation the signal is resampled giving 3000 samples from 100km down to 4km, of which only 100 is used in the range from 100 to 50km. Furthermore, because of the increasing density of the atmosphere of the Earth a large number of expansion functions are necessary to give an appropriate approximation of the phase with the given expansion functions. Thus, the least squares minimization problem has been solved using the Conjugate gradients least squares (CGLS) method.

To use the CGLS method on the given minimization problem (25) the problem must be transformed to standard form. As $\mathbf{L}$ is square and invertible the transformation is simple [Hansen, 1997, ch. 2.3]:

$$\overline{\left(\frac{\partial \mathbf{F}}{\partial \boldsymbol{\phi}} \right)} = \left(\frac{\partial \mathbf{F}}{\partial \boldsymbol{\phi}} \right) \mathbf{L}^{-1}, \quad \overline{(\boldsymbol{\upsilon} - \mathbf{F}[\boldsymbol{\phi}])} = (\boldsymbol{\upsilon} - \mathbf{F}[\boldsymbol{\phi}]), \quad \partial \boldsymbol{\phi} = \mathbf{L}^{-1} \overline{\partial \boldsymbol{\phi}} \tag{26}$$

giving the minimization problem

$$\min \left\{ \left\| \overline{\left(\frac{\partial \mathbf{F}}{\partial \boldsymbol{\phi}} \right)} \overline{\partial \boldsymbol{\phi}} - \overline{(\boldsymbol{\upsilon} - \mathbf{F}[\boldsymbol{\phi}])} \right\|_2^2 + \lambda^2 \left\| \overline{\partial \boldsymbol{\phi}} \right\|_2^2 \right\} \tag{27}$$

where $\mathbf{L}^{-1}$ is a diagonal matrix with the elements $\frac{1}{w_i}$.

The CGLS method is an iterative method for solving linear equations. When the CGLS method is used on a standard form problem the regularization is controlled by the number of iterations. The fewer the iterations the more regularization [Hansen, 1997, ch. 6.3].

3 Results

As example used to test the inversion method a simulated occultation data set has been used.

A one dimensional forward occultation simulator which takes into account diffraction has been developed at JPL, i.e., large gradients can be simulated. The model uses a spherical Earth, spherical satellite orbits and a piecewise linear temperature profile as atmosphere model [Kursinski et al., 1997]. Forward simulation data from this model has been provided by Roger E. Linfield and Rob Kursinski, JPL.

The approximations in this model compared to a real occultation are relatively small and the influence on the results are well known so when using the simulated data set a good test of the inversion method can be performed.

Figure 5 shows the temperature profile and the corresponding refractivity profile for the example used here. The refractivity N corresponds to the refractive index as

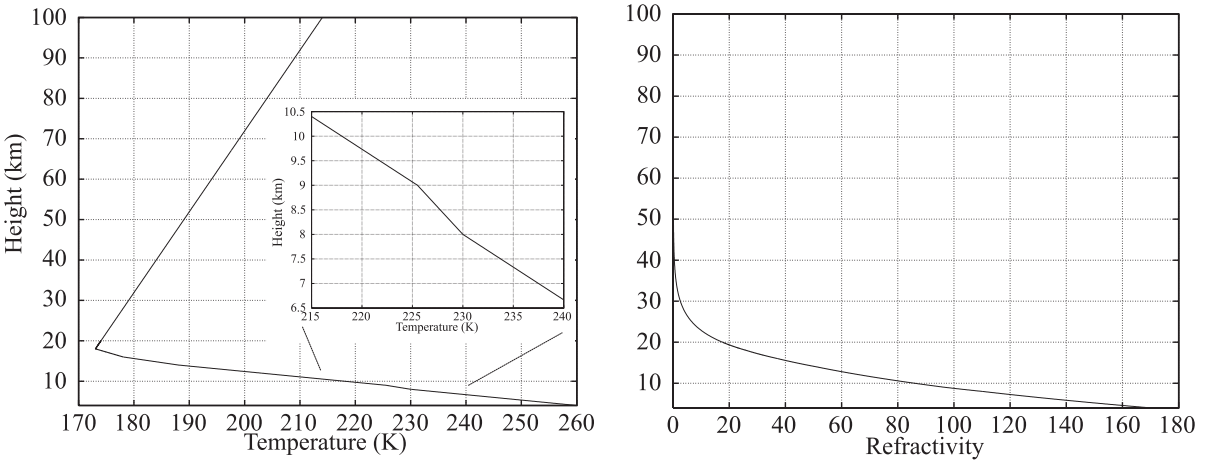

Figure 5: Temperature and refractivity profiles as a function of height for the example used.

$$N = (n - 1) \cdot 10^6. \tag{28}$$

Figure 6 shows the simulated occultation measurement as a function of the corresponding height in the atmosphere. The results shown has been obtained with the first screen placed at $z_1 = -50km$ and the second screen placed at $z_2 = 110km - 0.5\xi$. These positions of the screens gives the optimal results of the forward calculation using two thin screens. The measured amplitude is shown relative to the amplitude that would be measured in the absence of the atmosphere and the measured phase is similarly shown subtracted with the phase delay caused by the direct propagation in the case where there is no atmosphere. The oscillations in the amplitude are

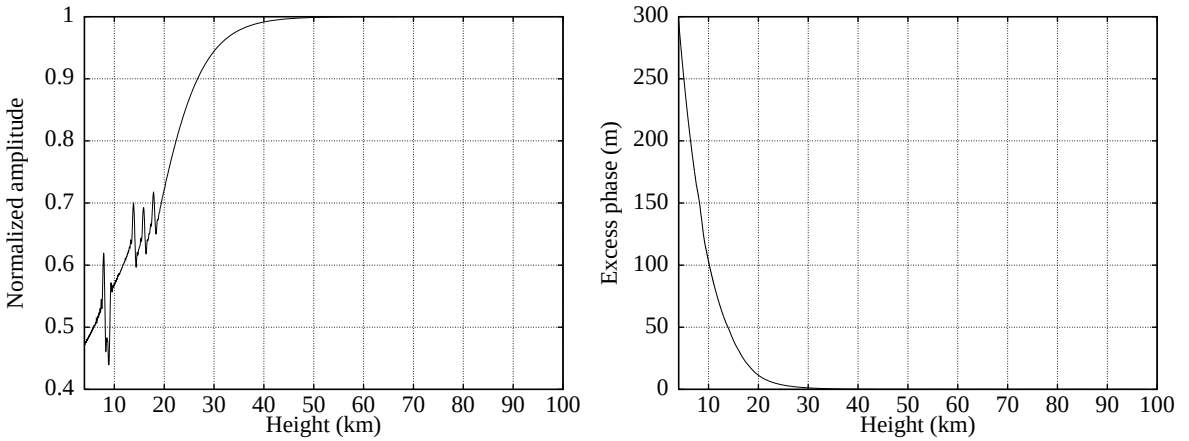

Figure 6: Measured amplitude and phase for the example used.

caused by changes in the temperature gradient. The slight change in the temperature gradient seen from 8-9km height in Figure 5 is seen to cause rather large oscillations in the measured amplitude. In general the oscillations increases as the gradient change increases but furthermore the oscillations increases as the gradient changes gets closer to the Earth. The temperature gradient changes also causes oscillations in the phase but due to the very fast increase of the phase below 20km the oscillations can not be distinguished as easily as in the amplitude. It should be noted, that the wavelength at the frequency used is approximately $0.2m$ so the excess phase shown is equal to $1500 \cdot 2\pi$ at the height $4km$.

3.1 Inversion Results

The inversion results in this section is only inversion to the phase delay Ψ due to the atmosphere. Once the Ψ has been found the inversion to refractivity using (9) is relatively simple to perform.

When inverting the data shown above an initial guess of the phase delay must be obtained. To obtain this guess, the traditionally used geometrical optics solution is used to invert the data to a refractivity profile and then the phase delay is calculated from (7). The phase delay thus obtained for each of the thin screens for the example used is shown in Figure 7. In the complex representation this phase delay will be $1 \cdot \exp(ik\psi)$. The geometrical optics solution is very good for smooth profiles. The example has a quite smooth profile which the geometrical optics solution can invert with very high accuracy so the initial guess should be pretty accurate. Discrepancies between the simulated measurement and the two thin screen propagator when using ψ in Figure 7 as initial guess will thus mainly be due to errors in the two thin screen approximation. But as the purpose is to derive the inversion result obtainable with the two

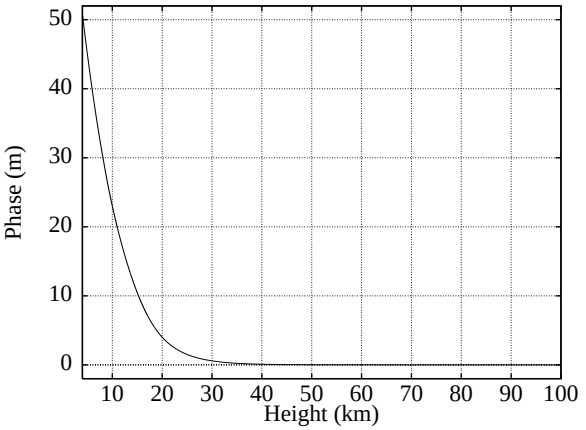

Figure 7: The phase delay corresponding to the refractivity profile derived using a geometrical optics solution for the example used.

thin screen approximation, iterations must be performed to obtain the phase delay result which complies best with the two thin screen method.

The error of the two thin screen propagation when using the phase delay shown in Figure 7 compared to the simulated measurement is shown in Figure 8. Both amplitude and phase errors

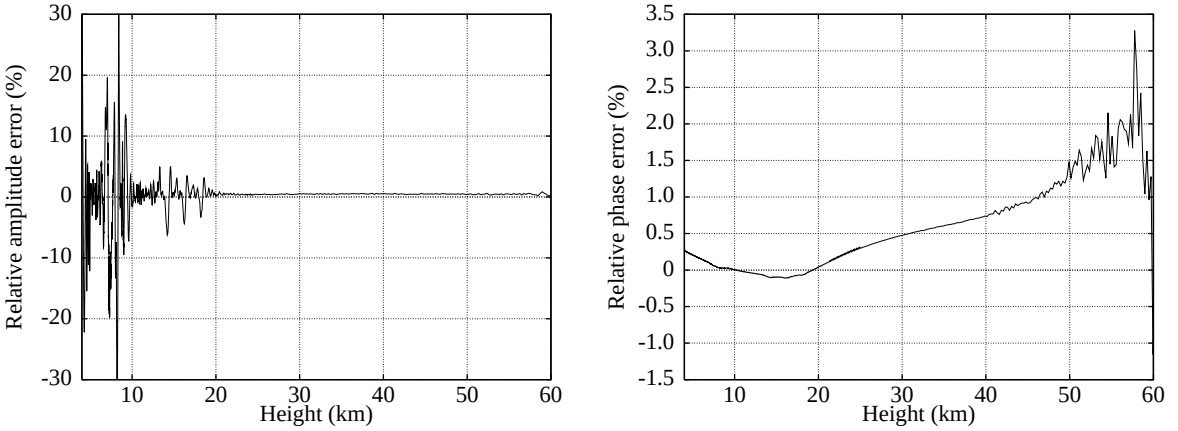

Figure 8: Relative errors in amplitude and phase using the initial phase delay guess.

are shown relative. The results are only shown below 60km. This is because the phase decreases exponentially giving accuracy problems for high altitudes. Normally only results below 30-40km are considered reliable no matter what inversion method is used. The high altitude are necessary though to initialize the algorithm.

The increasing errors in the phase above 40km is thus not a very big problem although better results should be obtainably. In absolute measures the error in the phase below 10km is a much bigger problem as the phase varies very fast in this area and even 0.25% errors are several periods of the complex phase. Below 30-40km the error should be less than $\approx 0.05\%$ in order to accept the result as converged. But still, the relatively small error in the phase with the initial guess implies that the results obtainable with the two thin screen method will have a reasonably good

average accuracy.

The errors in the amplitude increases as the altitude decreases. This is because the absolute amplitude decreases. Also, it is seen that the temperature gradient changes causes some problems for the amplitude results. The large errors seen in the amplitude results compared to the phase results are to be expected as any approximation of the wave propagation approximates the phase better than the amplitude. As only the phase is necessary to derive the refractive index profile this is not a problem for the further inversion process but it is likely to cause problems for the inversion to phase delay as this inversion can only be performed on the complex phase delay and thus will be influenced by both errors.

3.1.1 CGLS solution to the updating equations

The error in Figure 8 is used as right hand side in the updating equations (22) for the first iteration. Figure 9 shows the real and imaginary part of the right hand side as it look in absolute measures. The electromagnetic field has been normalized to the field which would have been measured in free space as in the figures shown previously. The right hand side contains

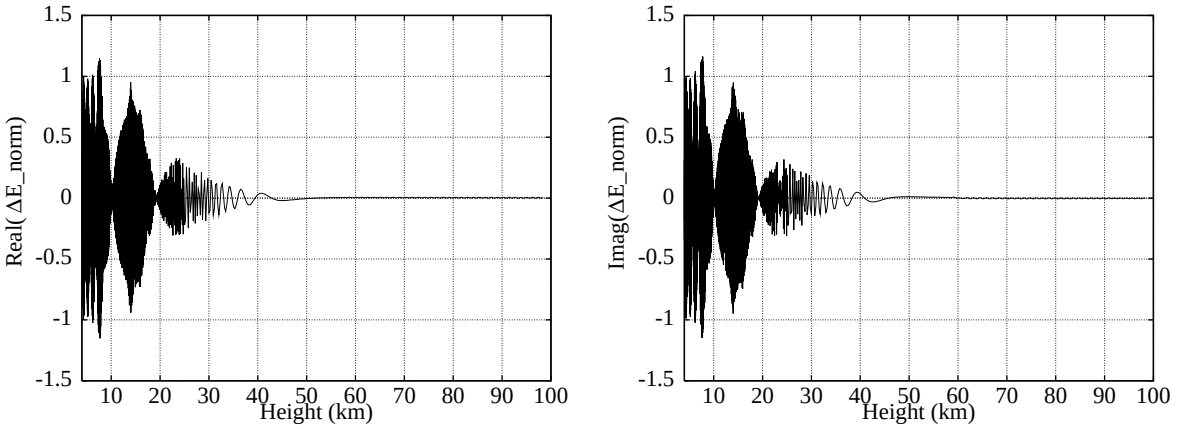

Figure 9: Real and imaginary part of errors in initial phase delay guess.

numerical noise. Due to accuracy problems in the calculation of the forward propagation the noise level in the right hand side is approximately $\|e\|_2 \approx 0.2$. This noise is a combination of model error and rounding error from numerical integrations. The noise is assumed to be uncorrelated although this is probably only approximately correct. The noise is particularly easy to see at high altitude, where amplitude and phase oscillations are obvious due to the relatively small influence from the atmosphere. The simulated occultation data set is assumed to be noise free.

The exact number of samples used are 3044 and the number of expansion functions used for the phase delay is 2456. In principle the updating matrix will be a full matrix as the measured field depends on field at any point of the thin screens. In practice the dependence is very concentrated around a center point so the matrix will be banded. The CGLS algorithm is initialized with the starting vector $d\phi^{(0)} = 0$.

In Figure 10 the L-curve for the CGLS solution of the updating equations is shown and Figure 11 shows the residual norm and the solution norm as a function of iteration number. The CGLS

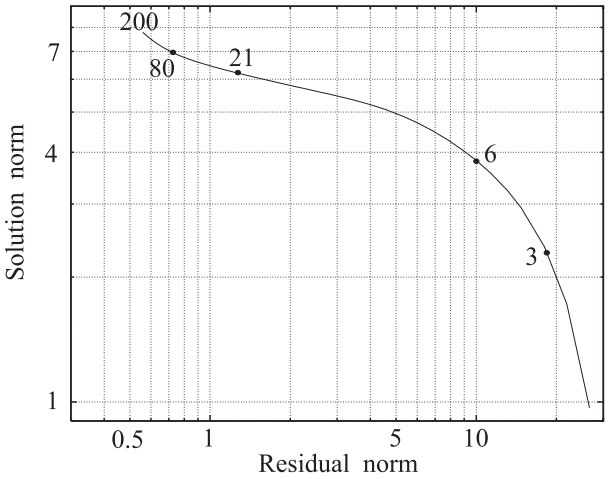

Figure 10: The L-curve

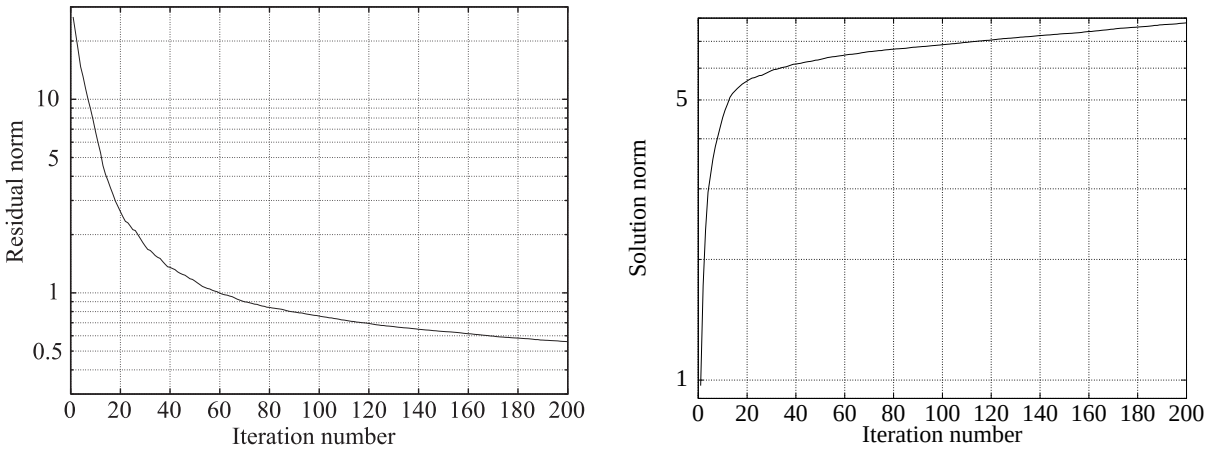

Figure 11: The development of the residual norm for the CGLS solution of the updating equations is shown on the left and on the right is the corresponding development of the norm of the solution.

iterations are stopped after 200 iterations. In Figure 10 the iteration number is shown in a few point. As can be seen from the figure the corner of the L-curve appears after approximately 80 iterations. The corner is placed well above the noise level in the right hand side but on the other hand the updating matrix is know to contain noise as well. Although it is difficult to estimate the noise level in the updating matrix it is expected that it will be substantially larger than the noise level in the right hand side as matrix is obtained by differentiation of the equations used for the forward propagation. The development of the residual norm shown in Figure 11 and the development of the error norm which is also shown in Figure 11 behaves as would be expected [Hansen, 1997, ch. 6.4].

In Figure 12 solutions corresponding to the iteration numbers marked in the L-curve is shown

with the exception that the corner solution has been substituted with the solution for iteration number 50. The figure shows the amplitude of the solution on the left and the unwrapped phase

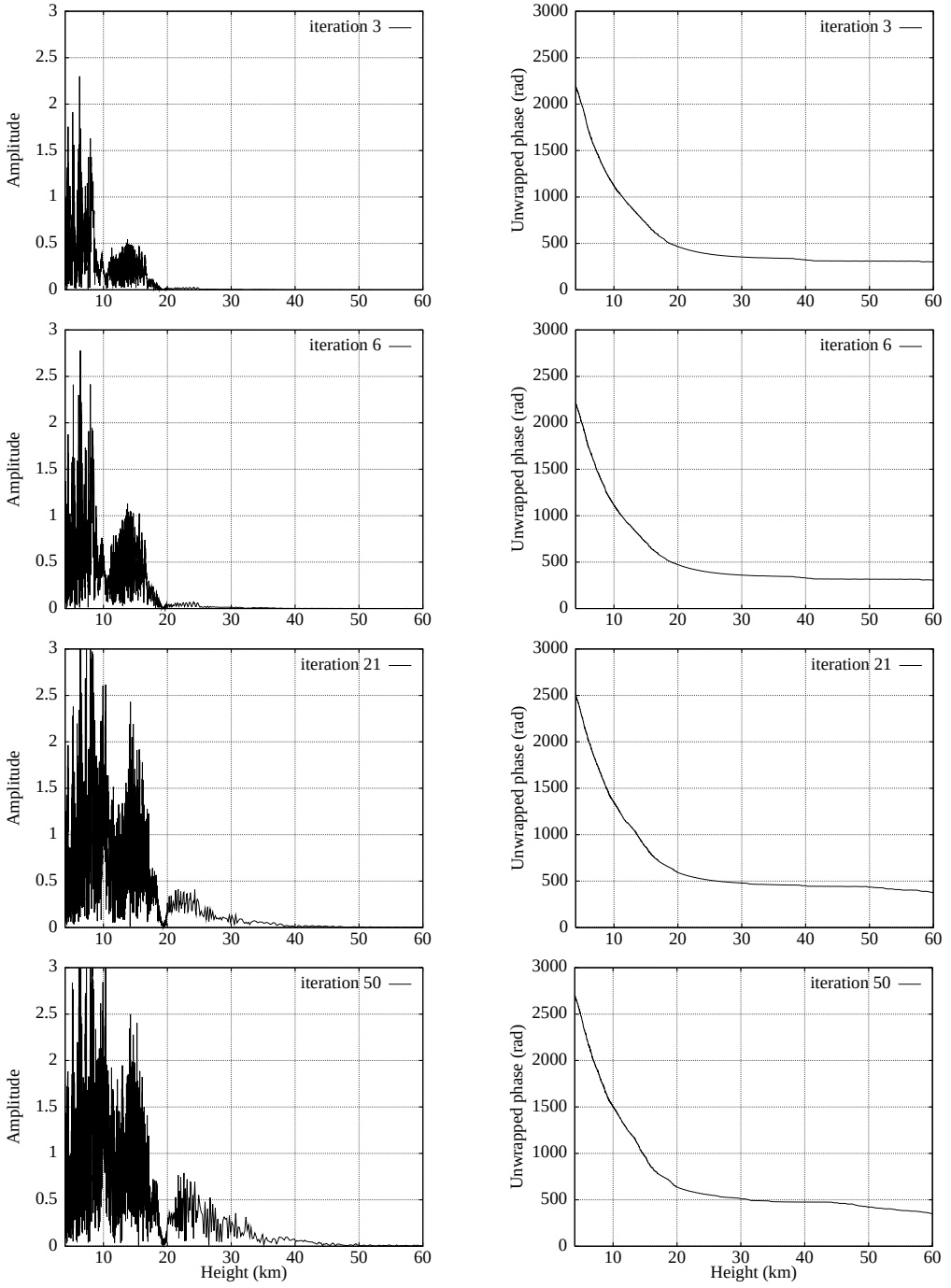

Figure 12: Phase and amplitude for different iteration numbers.

of the complex solution on the right. The figure shows that the results are rather noisy and furthermore, the noise is seen to increase a lot with iteration number. The solution is to be added to the initial phase guess and should compensate the error shown in Figure 8. From theoretical considerations and experience from single screen models it is known that the updating solution

should have a relatively constant amplitude with a maximum around 1. When the amplitude of the updating equation is larger than one the updating result will dominate the phase when added to the initial guess. Taking the very fast phase variations in the updating results into account it is seen that it will be necessary to chose a solution which when compared to the L-curve corner solution seems to be over-smoothed.

Use of a different smoothing norm in the minimization problem for the updating solution (25), i.e., $\|\mathbf{L}\partial\boldsymbol{\phi}\|_2^2$ instead of $\|\partial\boldsymbol{\phi}\|_2^2$ with $\mathbf{L}$ equal to the first derivative operator does improve the results significantly.

3.1.2 The updated phase

Instead of using the L-curve corner solution the solution to the updating equations has been chosen by trial and error. This process is equal to the finding the regularized solution in accordance with equation (16), i.e., finding the solution which minimizes the error of the forward propagator when the updated phase is used.

Figure 13 shows the error in the measured phase obtained with the two thin screen forward propagator with the updated phase using the solutions shown in Figure 12 for the updating. The results are shown together with the error obtained using the initial phase guess. It should

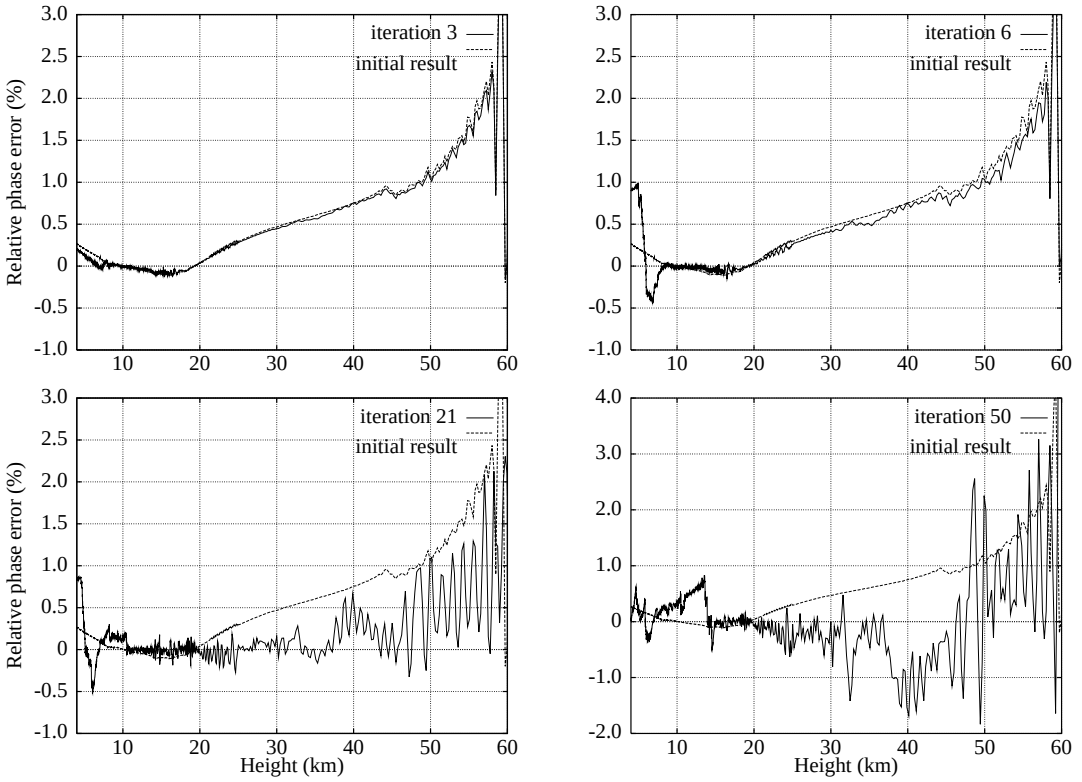

Figure 13: Relative phase errors when using different iteration numbers for the updating solution. In each plot the error obtained using the initial phase guess is shown for comparison.

be noted that the scale is different for the result obtained using the iteration number 50 in the updating. Only the phase error has been shown as this is the result which is important for finding the refractivity but also because amplitude and phase results are very closely connected. A small error in the phase will indicate a small error in the amplitude but with the complication that the amplitude is less accurate than the phase and will be very sensitive to noise particularly close to the Earth.

The figure shows - as would have been expected from Figure 12 - that the updating solutions corresponding to high iteration numbers only work well for high altitudes. As the Earth is approached the iteration number used for the solution to the updating must be lowered. The figure furthermore shows that the solution for iteration 50 is to noisy at any altitude and the average solution has started to give increasing errors. On the other hand using a low iteration number gives to small amplitudes of the updating equations for high altitudes, i.e., the updating makes no difference in the result. Therefore, the updating solution has been composed of a number of solutions corresponding to different numbers of CGLS iterations.

From 100km down to 50km the solution from the 21th iteration has been used. From 50km down to 10km the solution from iteration number 6 has been used and below 10km the solution from iteration number 3 has been used. The resulting updated complex phase delay Ψ is shown in Figure 14.

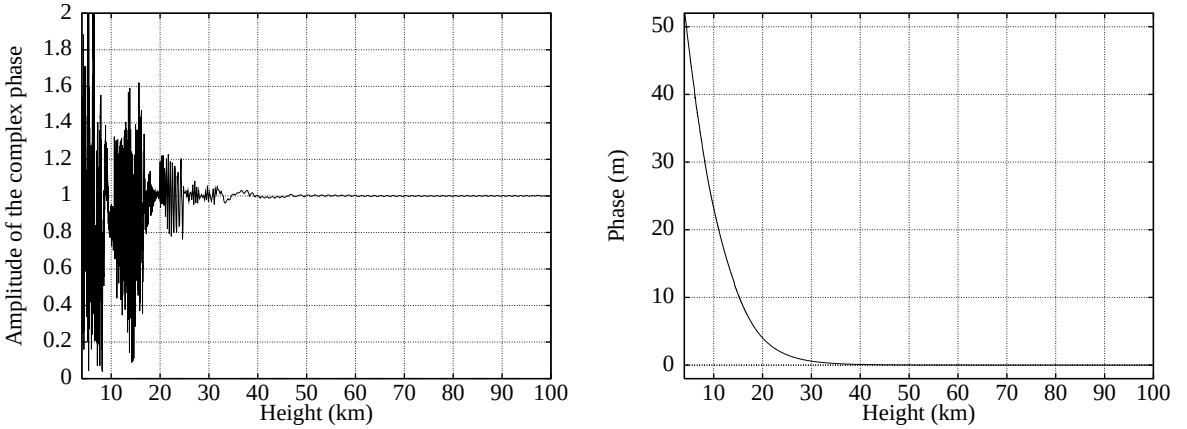

Figure 14: The complex phase after addition of initial data with updating results.

Even when a low iteration number is used for the solution below 50km the resulting amplitude is seen to be oscillating pretty much - compared to the initial amplitude of 1 constant. The updated phase delay ϕ which is shown on the right looks very reasonably compared to the original guess shown in Figure 7. It seems likely that an increased number of samples in the right hand side as well as an increased number of expansion function might help to minimize the problems with the solution below 10km but as the number of unknown is already rather large a further increase in the sampling density gives substantially computationally difficulties. This is because calculation of the matrix elements is a very slow process so the matrix elements should only be calculated once in order to keep the computational time reasonably.

The resulting updated complex phase is used in the two thin screen propagator. The error in the amplitude and phase compared to the simulated data set is shown in Figure 15. The figure

also shows the error obtained using the initial phase delay guess. As might have been expected

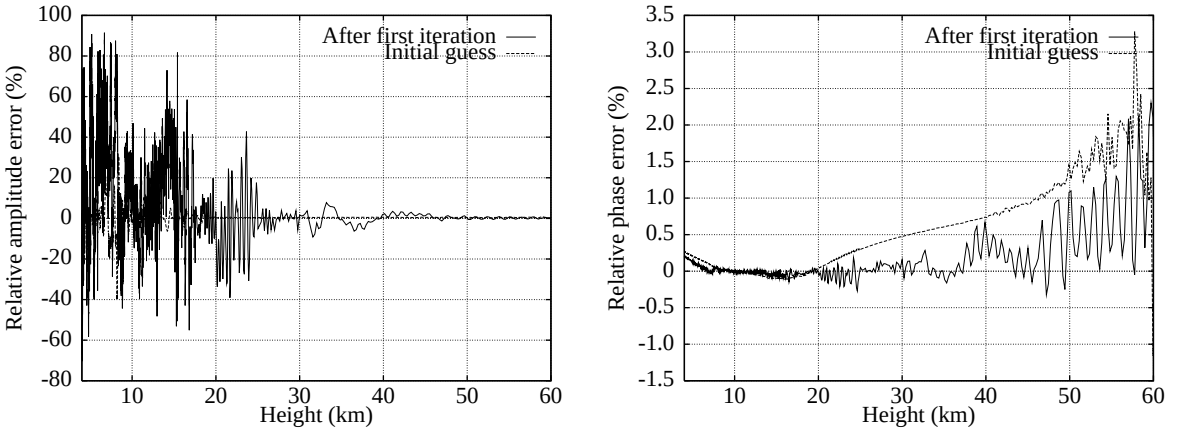

Figure 15: The relative error after first iteration shown together with the relative error after using the initial phase delay guess.

from the look of the updated complex phase the error in the amplitude is actually increases after this first iteration due to the large oscillations in the amplitude of the updated complex phase. On the other hand the relative phase error is decreased although there are oscillations in this result also.

The tendency of the updated solution to oscillate is both a result of the large right hand side of the updating equation and of the discretization errors in the matrix. That is, already the two thin screen propagation is seen to have a slight tendency to oscillate and as the matrix in the updating equation is derived from a differentiation of the forward propagation the problem is increased. Use of a smoothing operator L like a first order differentiation in the least squares solution (27) instead of just the simple weighting does not improve the results significantly.

The average of the phase almost fulfills the convergence criteria of an error less than 0.05% in the area below 30km. Below 7km the phase error still increases somewhat. But overall the error is decreased implying that the inversion method is feasible. Further iterations to improve the phase result below 7km is likely to be difficult due to the large oscillations in the amplitude results.

3.1.3 Further improvements of the results

The results shown uses only one iteration in the non linear iterative solution. In principle the error shown in Figure 15 could be used as right hand side for the updating equations in a new iteration. But due to the large noise level in the amplitude and the difficulties with noise in the updating equations this is not expected to give useful results.

It is known that the true solution to the inversion problem does not oscillate like the solution obtained using the nonlinear updating equation. Therefore, tests has been performed where a simple smoothing of the updated complex phase delay shown in Figure 14 has been applied before the two thin screen propagation is performed again. This process equals trying to find

the best solution to the regularized problem (16) with an empirical method. Even though the smoothing has not been optimized this seems to be a way of removing most of the unwanted oscillations in the results and giving the same average accuracy of the phase. Figure 16 show the error in the measured data when a smoothed version of the complex phase shown in Figure 14 has been used as the updated phase. The amplitude of the complex phase has been set to 1 constant and the high frequency oscillations in the phase of the complex phase has been removed. The result shown in Figure 16 is reasonably good for both the measured phase and amplitude.

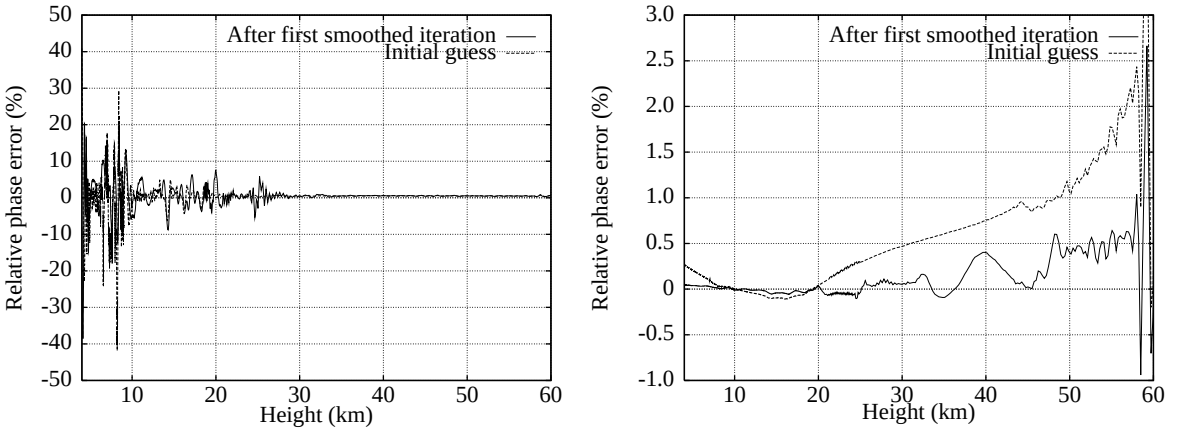

Figure 16: The relative error after first iteration using the smoothed updated phase shown together with the relative error after using the initial phase delay guess.

The figure shows that a part from giving noisy results the updating equations works for the non linear inversion. The results could be used for performing another iteration in the nonlinear inversion but below 35km the accuracy is approximately as required so another iteration has not been considered necessary.

4 Conclusions

The initial test results of the two thin screen inversion method shows that the nonlinear inversion method is feasible although it is computationally and implementationally demanding.

The method still needs a lot of development before it can be used in general even on simulated data without noise. Especially, work could be done on choosing better expansion function for the phase and finding better and more automated regularized solutions. But with an effort of making the implementation more efficient it is expected that very high resolution inversion results should be obtainable.

References

[Blok and Oristaglio, 1995] Blok, H. and Oristaglio, M. (1995). Wavefield imaging and inversion in electromagnetics and acoustics. Technical Report Rep. nr. eT/EM 1995-21, Centre for Technical Geoscience, Delft University of Technology.

[Born and Wolf, 1993] Born, M. and Wolf, E. (1993). *Principles of Optics.* Pergamon Press, Oxford, England, 6 edition.

[Hansen, 1997] Hansen, P. C. (1997). *Rank-Deficient and Discrete Ill-Posed Problems: Numerical Aspects of Linear Inversion.* SIAM monographs on mathematical modeling and computation. SIAM, Philadelphia, USA.

[Kursinski et al., 1997] Kursinski, E., Hajj, G., Hardy, K., Schofield, J., and Linfield, R. (1997). Observing earth's atmosphere with radio occultation measurementes using GPS. *J. Geophys. Res.*, 102(D19):23,429–23,465.

[Mortensen and Høeg, 1998] Mortensen, M. and Høeg, P. (1998). The fresnel transform for inversion of GPS occultations of the Earth's atmosphere. *GRL.*

[Syndergaard, 1998] Syndergaard, S. (1998). Modeling the impact of the earth's oblateness on the retrieval of temperature and pressure profiles from limb sounding. *Journal of Atmospheric and Solar-Terrestrial Physics*, Vol. 60(No. 2):pp. 171–180.

[Tartarskii, 1971] Tartarskii, W. I. (1971). *The effects of the Turbulent Atmosphere on Wave Propagation.* Natl. Tech. Inf. Serv., Springfield, Va.